INFECTION AND IMMUNITY, Sept. 2011, p. 3563–3575 Vol. 79, No. 9
0019-9567/11/$12.00 doi:10.1128/IAI.05175-11

Cholesterol Depletion Reduces Entry of *Campylobacter jejuni* Cytolethal Distending Toxin and Attenuates Intoxication of Host Cells[▽]

Chia-Der Lin,[1]†‡ Cheng-Kuo Lai,[2]† Yu-Hsin Lin,[3] Jer-Tsong Hsieh,[4] Yu-Ting Sing,[1] Yun-Chieh Chang,[5] Kai-Chuan Chen,[6] Wen-Ching Wang,[5] Hong-Lin Su,[2] and Chih-Ho Lai[1,4]*

School of Medicine and Graduate Institute of Basic Medical Science, China Medical University, Taichung, Taiwan[1]; Department of Life Sciences, National Chung Hsing University, Taichung, Taiwan[2]; Department of Biological Science and Technology, China Medical University, Taichung, Taiwan[3]; Department of Urology, University of Texas Southwestern Medical Center, Dallas, Texas[4]; Institute of Molecular and Cellular Biology, National Tsing Hua University, Hsinchu, Taiwan[5]; and Institute of Biomedical Sciences, Academia Sinica, Taipei, Taiwan[6]

Received 2 April 2011/Returned for modification 16 April 2011/Accepted 18 June 2011

***Campylobacter jejuni* is a common cause of pediatric diarrhea worldwide. Cytolethal distending toxin, produced by *Campylobacter jejuni*, is a putative virulence factor that induces cell cycle arrest and apoptosis in eukaryotic cells. Cellular cholesterol, a major component of lipid rafts, has a pivotal role in regulating signaling transduction and protein trafficking as well as pathogen internalization. In this study, we demonstrated that cell intoxication by *Campylobacter jejuni* cytolethal distending toxin is through the association of cytolethal distending toxin subunits and membrane cholesterol-rich microdomains. Cytolethal distending toxin subunits cofractionated with detergent-resistant membranes, while the distribution reduced upon the depletion of cholesterol, suggesting that cytolethal distending toxin subunits are associated with lipid rafts. The disruption of cholesterol using methyl-β-cyclodextrin not only reduced the binding activity of cytolethal distending toxin subunits on the cell membrane but also impaired their delivery and attenuated toxin-induced cell cycle arrest. Accordingly, cell intoxication by cytolethal distending toxin was restored by cholesterol replenishment. These findings suggest that membrane cholesterol plays a critical role in the *Campylobacter jejuni* cytolethal distending toxin-induced pathogenesis of host cells.**

Campylobacter jejuni is one of the most common causative agents of food-borne infectious illnesses in humans (10, 34). Inflammatory diarrhea is commonly seen in children infected with *Campylobacter* species (4, 47). Infection by the pathogen in humans usually occurs through the consumption of contaminated poultry products (13). However, the virulence factors responsible for the induction of host diarrhea remain unclear.

A bacterial membrane-associated protein, cytolethal distending toxin (CDT), has been identified as one of the virulence factors required for the induction of interleukin-8 (IL-8), which is a chemokine associated with local acute inflammatory responses (20, 59). CDT is a tripartite protein toxin composed of three subunits, CdtA, CdtB, and CdtC (28), encoded by an operon comprising *cdtA*, *cdtB*, and *cdtC* (46). Several bacterial species have been identified that contain CDT toxin, including *Aggregatibacter actinomycetemcomitans* (55), *C. jejuni* (22), *Escherichia coli* (45), *Haemophilus ducreyi* (12), *Helicobacter hepaticus* (58), and *Shigella dysenteriae* (41). CDT holotoxin functions as an AB_2 toxin in which CdtA and CdtC form a binding (B) unit and CdtB is an active (A) unit (27). A previous study demonstrated that CdtA and CdtC can interact with the cell membrane and enable the translocation of the holotoxin across the cell membrane (38). In addition, the nuclear-translocated CdtB subunit exhibits type I DNase activity, which causes DNA damage resulting in cell cycle arrest at the G_2/M phase (26).

Functional studies of CdtA and CdtC are relatively limited compared to those of CdtB. CdtA and CdtC adopt lectin-type structures that are homologous to ricin, a plant toxin (37, 38). The crystal structure of CDT from *H. ducreyi* revealed that it contains two important binding elements: an aromatic patch in CdtA and a deep groove at the interface of CdtA and CdtC (38). A structure-based mutagenesis study further demonstrated that mutations of the aromatic patch or groove impair toxin binding to the cell surface and reduce cell intoxication (39). The analysis of CDT from *A. actinomycetemcomitans* also revealed that CdtA and CdtC not only bind to the cell surface but also are associated with membrane lipid rafts (5). Lipid rafts are microdomains that contain large fractions of cholesterol, phospholipids, and glycosylphosphatidylinositol-anchored proteins (9, 21). *In vitro* studies showed that the structure of lipid rafts is stabilized in cold nonionic detergents such as Triton X-100 (8) but can be disrupted by the cholesterol depletion agent methyl-β-cyclodextrin (MβCD) (54). A recent study of *A. actinomycetemcomitans* CDT revealed that the

* Corresponding author. Mailing address: School of Medicine and Graduate Institute of Basic Medical Science, China Medical University, No. 91 Hsueh-Shih Road, Taichung, 40402 Taiwan. Phone: 886-4-22052121, ext. 7729. Fax: 886-4-22333641. E-mail: chl@mail.cmu.edu.tw.

† These authors contributed equally to this work.

‡ Present address: Department of Otolaryngology and Medical Education, China Medical University Hospital, and Graduate Institute of Clinical Medical Science, China Medical University, Taichung, Taiwan.

▽ Published ahead of print on 5 July 2011.

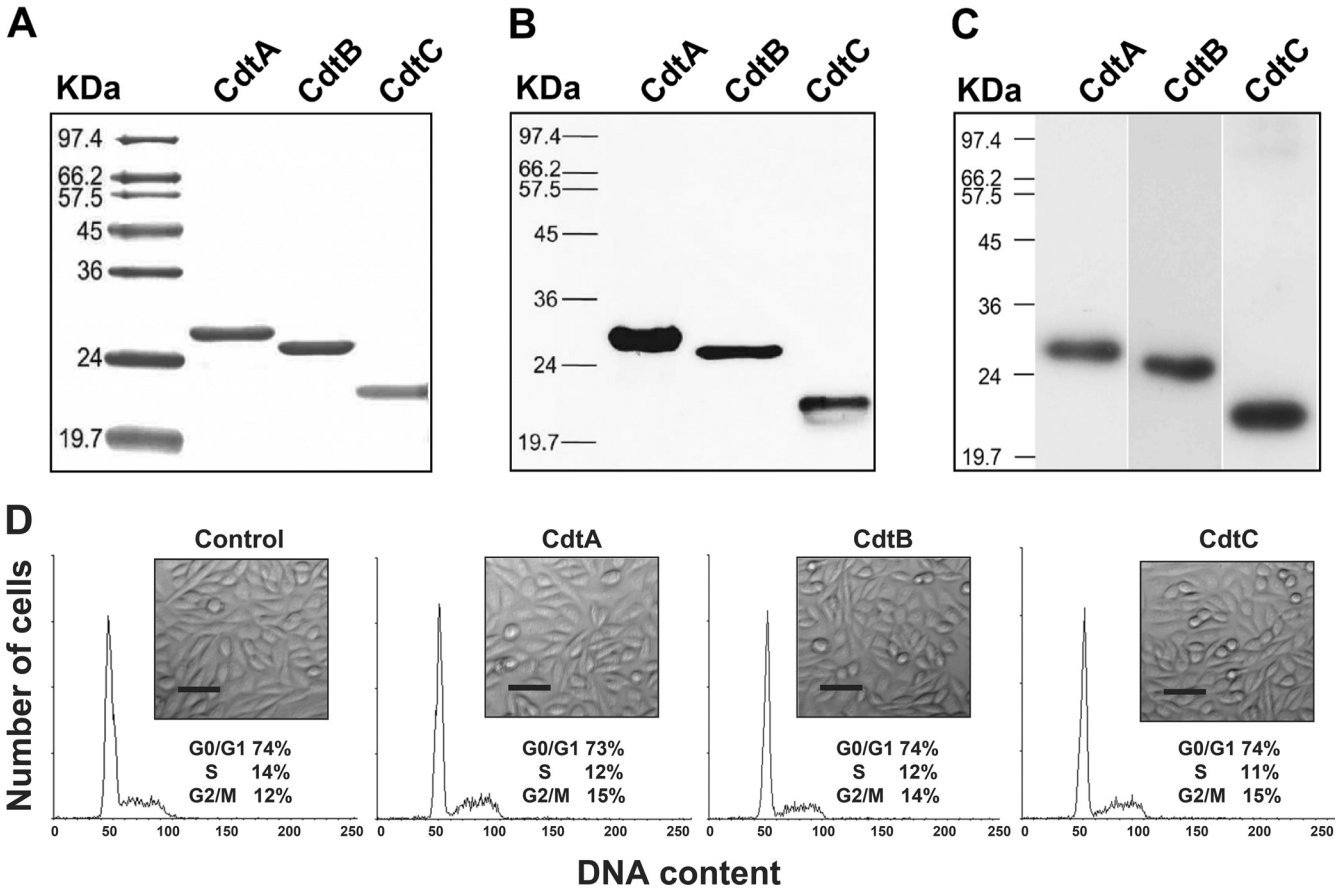

FIG. 1. Purification and characterization of each recombinant *C. jejuni* CDT subunit. (A) CDT proteins were expressed and purified as described in Materials and Methods. Each CDT subunit (2 μg/ml) was subjected to SDS-PAGE and stained with Coomassie brilliant blue. (B) Recombinant CDT protein (2 μg/ml) was loaded into each lane and verified by Western blot analysis with a monoclonal antibody specific to the His tag. (C) Western blot analysis was conducted on extracts of CHO-K1 cells exposed to the CDT holotoxin and assessed by antisera against CdtA, CdtB, or CdtC. Molecular mass markers (kDa) are shown on the left. (D) CHO-K1 cells were untreated (control) or treated with 200 nM each purified recombinant subunit at 37°C for 48 h. The cells then were examined under an inverted optical microscope to assess the effects of each CDT subunit. The cell cycle distribution was based on the DNA content, which was determined by flow cytometry. The percentage of cells in the G_0/G_1, S, and G_2/M phases of the cell cycle are indicated below the insets. Scale bar, 50 μm. The results represent one of three independent experiments.

CdtC subunit contains a cholesterol recognition/interaction amino acid consensus (CRAC) region, which is required for CdtC binding to cholesterol-rich microdomains (6). This finding indicates that cholesterol provides an essential ligand for CDT binding to the cell membrane and also serves as a portal for CdtB delivery into host cells for the induction of cell intoxication.

A growing number of studies have reported that some pathogens exploit lipid rafts for toxin delivery to induce host pathogenesis (1, 5, 19, 25, 48). However, the interaction between *C. jejuni* CDT subunits and membrane cholesterol-rich microdomains, as well as the role of cholesterol in the CDT intoxication of host cells, are largely unknown. In the present study, we propose that the association of *C. jejuni* CDT subunits with the host membrane is mediated in a cholesterol-dependent manner. Biochemical and cellular studies as well as confocal microscopy were used to explore the association of CdtA and CdtC with membrane lipid rafts. The binding of CDT subunits to the cell membrane, nuclear delivery of CdtB, and G_2/M arrest were reduced when cellular cholesterol was depleted. Our results provide evidence that membrane cholesterol plays an essential role in the binding of *C. jejuni* CDT subunits to membrane rafts, which promotes the pathogenic events in host cells.

MATERIALS AND METHODS

Reagents and antibodies. Anti-His (His probe) and anti-proliferating cell nuclear antigen (anti-PCNA) were purchased from Santa Cruz Biotechnology (Santa Cruz, CA). Anti-caveolin-1 and anti-transferrin receptor (anti-CD71) were purchased from BD Pharmingen (San Jose, CA). Anti-actin mouse monoclonal antibodies were purchased from Upstate Biotechnology (Lake Placid, NY). Alexa Fluor 647-conjugated anti-rabbit IgG and 4′,6′-diamidino-2-phenylindole (DAPI) were purchased from Molecular Probes (Invitrogen, Carlsbad, CA). ICRF-193 was purchased from Sigma-Aldrich (St. Louis, MO). MβCD, a cholesterol depletion agent which is commonly utilized to extract eukaryotic cholesterol from lipid rafts (53), was purchased from Sigma-Aldrich.

Bacterial and cell models. *C. jejuni* strain 7729, isolated from patients' feces, was identified and deposited at the Chang Gung Memorial Hospital (Taoyuan, Taiwan) (57). The bacterial strain was grown on Brucella blood agar plates (Becton Dickinson, Franklin Lakes, NJ) supplemented with 10% sheep blood and 1.5% agar in a microaerophilic atmosphere at 37°C for 1 to 2 days. CHO-K1 cells (Chinese hamster ovary cells; CCL-61; American Type

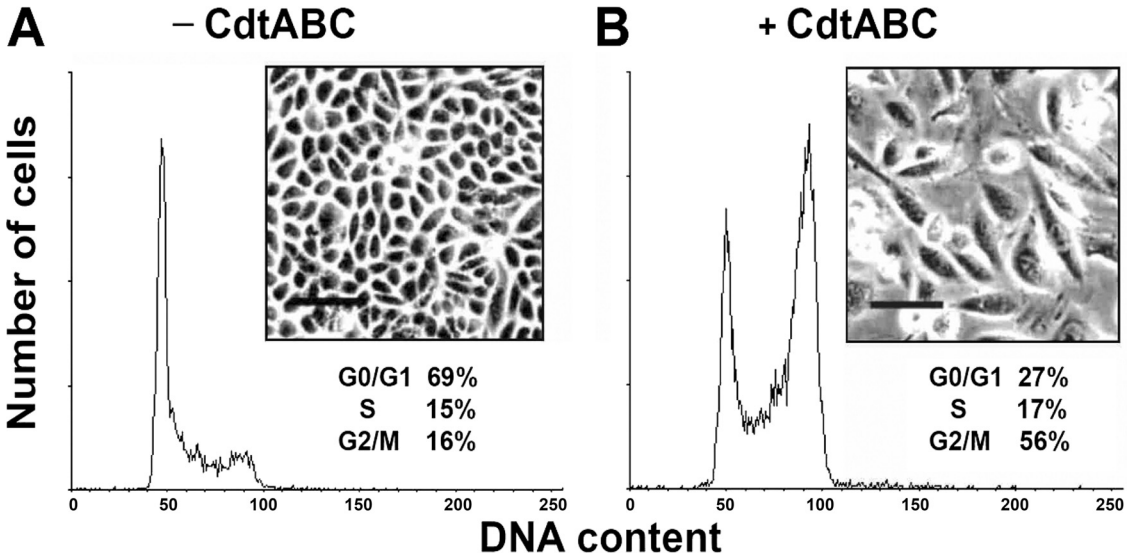

FIG. 2. Cell-distending activity of recombinant *C. jejuni* CDT subunits in CHO-K1 cells. CHO-K1 cells were left untreated (A) or treated with *C. jejuni* CDT holotoxin (CdtA, CdtB, or CdtC; 200 nM each subunit) (B) for 48 h at 37°C. The cells then were examined under an inverted optical microscope to assess the effects of CDT intoxication. Scale bar, 100 μm. The cell cycle distribution was based on the DNA content, which was determined by flow cytometry. The percentages of cells in the G_0/G_1, S, and G_2/M phases of the cell cycle are indicated below the insets. The results represent one of three independent experiments.

Culture Collection, Manassas, VA) and AGS cells (human gastric adenocarcinoma cells; CRL-1739) were cultured in F12 medium (HyClone, Logan, UT). COLO205 cells (human colon adenocarcinoma cells; CCL-222) and Caco-2 cells (human colon adenocarcinoma cells; HTB-37) were cultured in RPMI 1640 medium (Invitrogen). All cell culture media were supplemented with 10% fetal bovine serum (FBS) (HyClone) and penicillin and streptomycin (Invitrogen).

Construction and protein purification of CDT subunits. Recombinant His-tagged CDT subunits were cloned by following standard protocols. DNA fragments of *cdtA*, *cdtB*, and *cdtC* were derived from the PCR amplification of *C. jejuni* 7729 genomic DNA. The forward and reverse oligonucleotide primers were cdtA-F (CATGCCATGGCTTGTTCTTCTAAATTTGAAAATGT) and cdtA-R (CCGCTCGAGTCGTACCTCTCCTTGGCGATATA) for the PCR amplification of the *cdtA* sequence, cdtB-F (CATGCCATGGCTAATTTAGA AAATTTTAATGTTGGC) and cdtB-R (CCGCTCGAGAAATTTTCTAAAA TTTACTGGAAA) for the *cdtB* sequence, and cdtC-F (CATGCCATGGCTA CTCCTACTGGAGATTTGAAAGA) and cdtC-R (CCGCTCGAGTT CTAA AGGGGTAGCACTG) for the *cdtC* sequence. Each *cdt* fragment was inserted into pET21d (Invitrogen, Carlsbad, CA) using NcoI and XhoI. Briefly, *cdtA* was amplified using primers cdtA-F and cdtA-R by PCR at 95°C for 10 min for 1 cycle; 35 cycles at 95°C for 1 min, 55°C for 1 min, and 72°C for 2 min; and a final extension at 72°C for 20 min. The NcoI/XhoI fragment then was ligated with pET21d to create the CdtA expression plasmid. Similar protocols were used to obtain the CdtB and CdtC expression plasmids from *C. jejuni* 7729 using primer pairs cdtB-F/cdtB-R and cdtC-F/cdtC-R, respectively. The PCR program used to amplify *cdtB* and *cdtC* were the same as that for *cdtA*. The nucleotide sequence of each *cdt* construct was verified using the ABI Prism Dye Terminator cycle sequencing ready reaction kit (Perkin-Elmer Corp., Norwalk, CT) in an automated DNA sequencer (model 377-96; Perkin-Elmer Corp.). Sequence analysis was performed by the University of Wisconsin Genetics Computer Group (Mad-

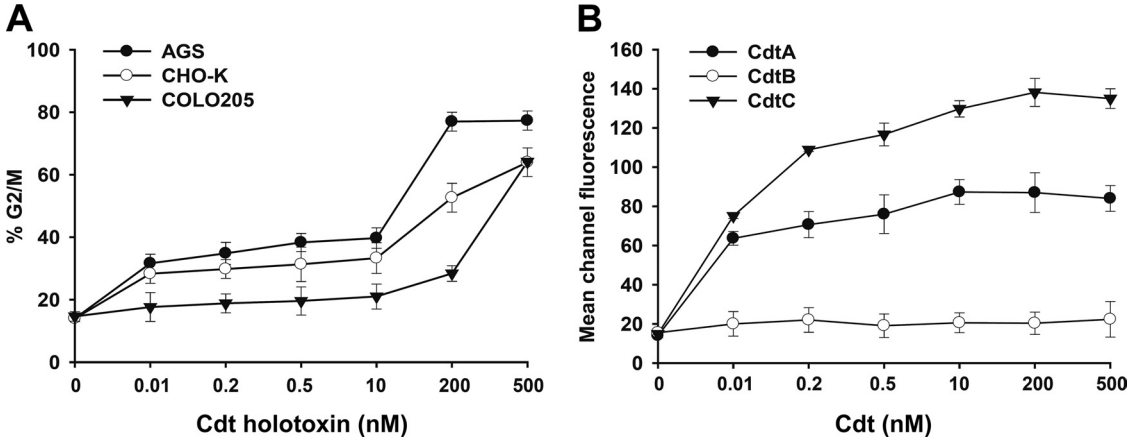

FIG. 3. CDT intoxication and binding of cells. (A) Cells from the indicated lines were treated with various concentrations of CDT holotoxin (0.01 to 500 nM) and incubated at 37°C for 48 h. Cell cycle distribution was based on the DNA content, which was determined using flow cytometry. The percentage of cells in the G_2/M phase was calculated. (B) CHO-K1 cells were exposed to each CDT subunit at the indicated concentrations (0.01 to 500 nM) and incubated at 4°C for 2 h. The cells were stained with individual antiserum against each CDT subunit followed by staining with FITC-conjugated anti-mouse IgG. The binding activity of each CDT protein was assessed by flow cytometry for FITC fluorescence. The results represent the means and standard deviations from three independent experiments.

ison, WI) package. *Escherichia coli* BL21(DE3) cells harboring either *cdtA*, *cdtB*, or *cdtC* expression plasmid was induced at an optical density at 600 nm (OD_{600}) of 0.8 by 0.5 mM isopropyl β-D-thiogalactopyranoside (IPTG) at 37°C for 3 h. The expressed His-tagged CdtA, CdtB, and CdtC fusion proteins were purified by metal affinity chromatography (Clontech, Palo-Alto, CA) and assessed by SDS-PAGE.

Generation of antiserum against each CDT subunit. Each purified CDT subunit (1 μg) was used to immunize a 6-week-old BALB/c mouse. All of the mice were purchased from the National Laboratory Animal Center (Taipei, Taiwan). The mice were immunized at weeks 0, 2, 4, 6, 8, 10, and 12, and the titer of the antiserum was detected at weeks 7, 9, 11, and 13. Mice were maintained in the animal center of China Medical University (Taichung, Taiwan). All procedures were performed according to the "Guide for the Care and Use of Laboratory Animals" (National Research Council) and were approved by the animal experiment committee of China Medical University (Taichung, Taiwan). The titers of antibodies against the CDT subunits in the serum were determined by enzyme-linked immunosorbent assay (ELISA). Ninety-six-well plates were coated with 500 ng of purified recombinant CDT subunits and blocked with 2% bovine serum albumin (BSA) in TBS (0.1 M Tris-HCl, pH 7.5, 0.03 M NaCl). Serial dilutions of the antiserum (1:1,000, 1:2,000, 1:4,000, 1:8,000, and 1:16,000) in TBS-Tween 20 were added to each well. Bound antibody was detected by horseradish peroxidase (HRP)-conjugated secondary antibodies (Invitrogen) and quantified by measuring the optical density at 450 nm after development with the TMB substrate buffer system (Kirkegaard & Perry Laboratories, Gaithersburg, MD).

SDS-PAGE and Western blot analysis. CDT holotoxin-treated cells were washed three times with phosphate-buffered saline (PBS) and then boiled in SDS-PAGE sample buffer for 5 min. The samples then were resolved by 12% SDS-PAGE and transferred onto polyvinylidene difluoride membranes (Millipore, Billerica, MA). The membranes were incubated with antiserum against each CDT subunit and then incubated with HRP-conjugated secondary antibodies (Invitrogen). The proteins of interest were visualized using the ECL Western blotting detection reagents (GE Healthcare, Piscataway, NJ) and detected using X-ray film (Kodak, Rochester, NY).

Cytolethal distending phenotype. CHO-K1 cells were cultured at 37°C for 20 h in six-well plates containing F12 medium supplemented with 10% FBS. After one wash with PBS, cells were exposed to an individual recombinant CDT subunit (200 nM) or CDT holotoxin (200 nM each subunit) for 48 h. The CDT-treated cells were observed using an inverted optical microscope (Carl Zeiss, Göttingen, Germany).

Flow cytometry analysis of cell cycle. CHO-K1 cells treated with CDT holotoxin were analyzed by flow cytometry. Cells were pretreated with MβCD (Sigma-Aldrich) for 1 h, washed, and exposed to CDT holotoxin or an individual CDT subunit for an additional 48 h. Cells were harvested and fixed with ice-cold 70% ethanol for 1 h and stained with 20 μg/ml propidium iodide (Sigma-Aldrich) containing 1 mg/ml RNase (Sigma-Aldrich) for 1 h. The stained cells were analyzed with an FACSCalibur flow cytometer (Becton Dickinson, San Jose, CA). The data were collected using 20,000 cells from each sample and analyzed using Cell Quest software WinMDI (Verity Software House, Topsham, ME). All samples were examined in triplicate from at least three independent experiments; all data are representations of typical experimental outcomes.

Detection of cellular cholesterol and cell viability assay. To measure the cholesterol levels in total cell lysates or detergent-resistant membrane (DRM), CHO-K1 cells were treated with various concentrations of MβCD. After incubation at 37°C for the indicated periods, the treated cells were washed three times with PBS and then disrupted by ultrasonication (three 10-s bursts at room temperature). The cholesterol content then was measured using an Amplex Red cholesterol assay kit (Molecular Probes, Eugene, OR). The percentage of remaining cholesterol after pretreatment with MβCD was determined as (fluorescence of treated cells obtained from a standard curve/total fluorescence of untreated cells) × 100 as previously described (25). To test the influence of MβCD on cell viability, cells were incubated with various concentrations of MβCD at 37°C for 1 h. After that, cells were washed three times with PBS and then incubated with fresh medium containing 10 μM lovastatin (Sigma-Aldrich) to inhibit cellular cholesterol biosynthesis. After incubation for a further 24 h, the viability of cells was determined by using a trypan blue exclusion assay. In brief, equal volumes of 0.2% trypan blue (Sigma-Aldrich) and cell suspension were mixed. A volume of 10 μl of the mixture was placed on the hemocytometer for counting trypan blue-stained cells. A total of 300 cells in randomly selected fields were counted by a light microscope. The percentages of live and dead cells were calculated as cell viability (percent) = (live cell count/total cell count) × 100. The analysis was examined in three independent studies, each conducted in duplicate.

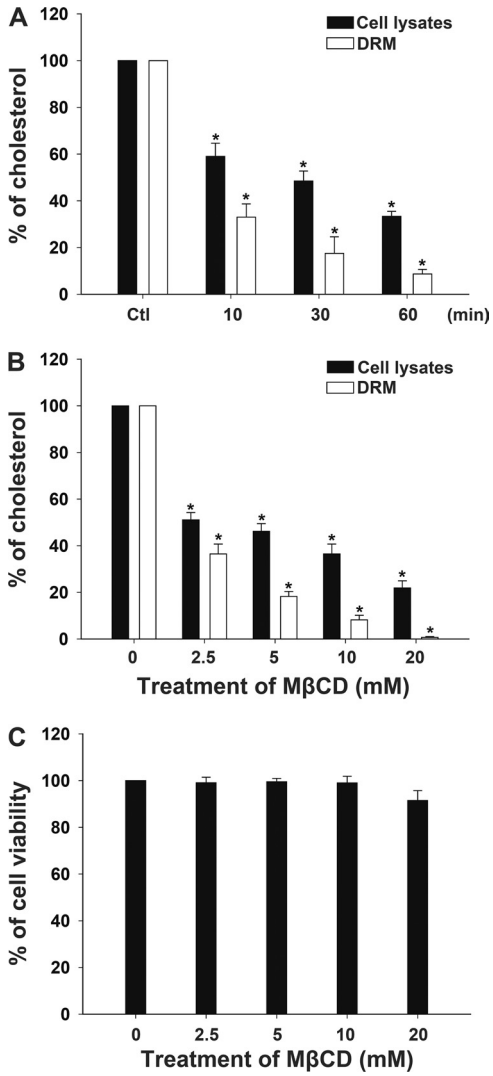

FIG. 4. Cholesterol depletion in CHO-K1 cells by treatment with MβCD. (A) CHO-K1 cells were treated with 10 mM MβCD at 37°C and incubated for the indicated times. The cells were harvested and subjected to cold detergent extraction using 1% Triton X-100, followed by centrifugation to isolate the DRM fraction. The prepared total cell lysates and DRM fraction then were analyzed for cholesterol concentration as described in Materials and Methods. (B) CHO-K1 cells were treated with various concentrations of MβCD (0, 2.5, 5, 10, and 20 mM) for 1 h. Whole-cell lysates and the DRM fraction then were prepared for cholesterol level analysis. (C) Cell viability was barely influenced after treatment with 0 to 20 mM MβCD, as determined by the trypan blue exclusion assay. The data represent the means and standard deviations from three independent experiments. An asterisk indicates $P < 0.05$ compared to results for each untreated control group, as determined by Student's *t* test. DRM, detergent-resistant membrane; MβCD, methyl-β-cyclodextrin.

Immunofluorescence labeling of CDT-treated cells. To visualize the localization of CDT in cells, CHO-K1 cells (0.5×10^6) were seeded on coverslips in six-well plates and incubated for 20 h. Cells were cultured with an individual CDT subunit (200 nM) or CDT holotoxin (200 nM each subunit) at 11°C for 1 h to maintain the fluidity of cell membrane and to prevent the internalization of cells (24). The cultured cells then were washed three times with PBS and fixed with 3.7% paraformaldehyde (Sigma-Aldrich) for 1 h. The cells were permeabilized with 0.1% Triton X-100 for 30 min and stained with anti-caveolin-1 antibody (BD Pharmingen), followed by being stained with Alexa Fluor 647-conju-

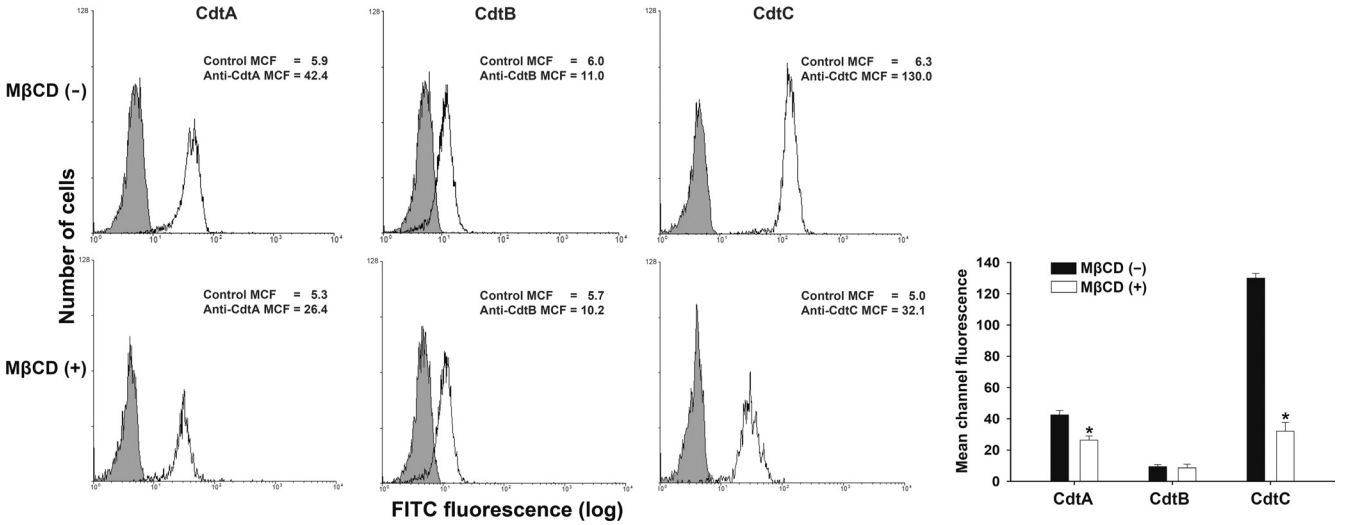

FIG. 5. Sufficient cellular cholesterol is essential for CdtA and CdtC binding to CHO-K1 cells. The cells were left untreated (upper) or treated with 10 mM MβCD (lower) for 1 h at 37°C, followed by exposure to 200 nM the individual recombinant *C. jejuni* CDT proteins. After incubation with the individual CDT proteins for 2 h at 4°C, the cells were stained with control preimmune serum or individual antiserum against each CDT subunit and stained with FITC-conjugated anti-mouse IgG. Binding activity was assessed by flow cytometry. The numbers represent the mean channel fluorescence (MCF). The quantitative data represent the means and standard deviations from three independent experiments and are shown in the lower right panel. Statistical analysis was calculated using Student's *t* test compared to each untreated MβCD group. An asterisk indicates statistical significance ($P < 0.05$).

gated anti-rabbit IgG (Molecular Probes). To label the individual CDT subunit, samples were incubated for 30 min with anti-CdtA, anti-CdtB, or anti-CdtC antiserum followed by fluorescein isothiocyanate (FITC)-conjugated AffiniPure goat anti-mouse IgG (Jackson ImmunoResearch, West Grove, PA). Samples were analyzed under a confocal laser-scanning microscope (Zeiss LSM 510; Carl Zeiss, Göttingen, Germany) with a 100× objective (oil immersion; aperture, 1.3). The distribution of fluorescence intensity for each CDT subunit and caveolin-1 was analyzed by ZEN software (Carl Zeiss) and schemed as line intensity histograms.

Isolation and analysis of DRM fraction. To isolate detergent-soluble and detergent-resistant fractions, CDT-treated cells were lysed with ice-cold TNE buffer (25 mM Tris-HCl, pH 7.5, 150 mM NaCl, 5 mM EDTA) containing 1% Triton X-100 and incubated on ice for 30 min. Cell lysates were centrifuged at 18,000 × *g* at 4°C for 30 min to separate the detergent-soluble and detergent-resistant fractions as described previously (53). Each fraction then was analyzed by Western blotting.

Isolation of nuclear fractions. To study the localization of CdtB in the nucleus of target cells, CHO-K1 cells were incubated in the presence or

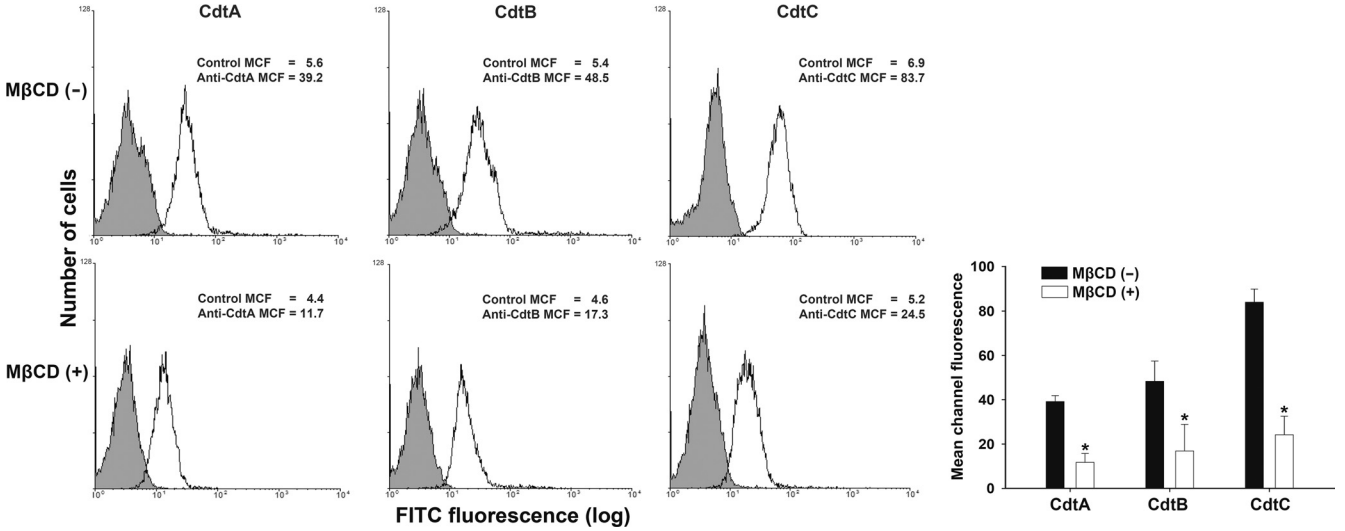

FIG. 6. Depletion of cholesterol reduces CDT holotoxin binding to cells. CHO-K1 cells were left untreated (upper) or treated with 10 mM MβCD (lower) for 1 h at 37°C prior to incubation with CDT holotoxin (200 nM). After incubation for 2 h at 4°C, the cells were probed with control preimmune serum or individual antiserum against each CDT subunit and stained with FITC-conjugated anti-mouse IgG. The level of binding activity was analyzed by flow cytometry for FITC fluorescence. The results represent the means and standard deviations from three independent experiments. The lower right panel shows the quantitative data of the CDT binding activity. An asterisk indicates significance compared to results for each untreated MβCD group, as determined by Student's *t* test ($P < 0.05$).

absence of 10 mM MβCD at 37°C. After 1 h, cells were exposed to CDT holotoxin at 37°C for the indicated periods. The nuclear proteins then were prepared using a nuclear extraction kit (Pierce, Rockford, IL). All protein concentrations were determined by colorimetric assay using the Bio-Rad assay kit (Bio-Rad, Hercules, CA). The isolated proteins (20 μg) from the nuclear fractions then were subjected to Western blotting for further analysis of CdtB localization.

Statistical analysis. The Student's *t* test was used to calculate the statistical significance of experimental results between two groups. $P < 0.05$ was considered statistically significant.

Nucleotide sequence accession numbers. The nucleotide sequences of *cdtA* and *cdtC* have been submitted to GenBank under accession numbers JF520784 and JF682840, respectively.

RESULTS

Expression and functional analysis of recombinant *C. jejuni* CDT subunits. We first investigated the activity of recombinant *C. jejuni* CDT using Chinese hamster ovary (CHO-K1) cells. Each *C. jejuni* CDT subunit was cloned and expressed with a His tag in *E. coli* BL21(DE3) cells. Recombinant CDT subunits then were purified and analyzed by SDS-PAGE (Fig. 1A). The purified recombinant CDT subunits were readily detected by Western blot analysis using a monoclonal anti-His antibody (Fig. 1B). Western blotting was carried out to determine whether polyclonal antibodies generated against each subunit could recognize the individual CDT subunits when they were assembled and associated with cells. As shown in Fig. 1C, the individual recombinant CDT proteins were recognized by the respective polyclonal CDT antiserum (anti-CdtA, anti-CdtB, or anti-CdtC). Thus, the polyclonal antisera were further applied to investigate the association of the CDT subunits with cell membrane lipid rafts. To characterize the biological function of *C. jejuni* CDT holotoxin, we examined its ability to induce cell distention in CHO-K1 cells. Our results revealed that no individual recombinant CDT protein had any effect on the cell cycle or the morphology of CHO-K1 cells after coculture for 48 h (Fig. 1D). However, upon the exposure of the cells to CDT holotoxin (200 nM each subunit) for 48 h, cell cycle analysis showed G_2/M arrest, and light microscopy indicated cell distention (Fig. 2).

To test whether CDT has the ability to intoxicate other cell types, we employed three different cell lines (AGS, CHO-K1, and COLO205 cells) to determine the intoxication activity of CDT. Each cell line was treated with various concentrations of CDT, and the cell cycle distribution was analyzed by flow cytometry. As shown in Fig. 3A, CDT-induced cell cycle arrest at the G_2/M phase in these three cell lines occurred in a dose-dependent manner. The saturation dose of CDT in AGS was ~200 nM. In contrast, the saturation doses of CDT in CHO-K1 and COLO205 cell lines were even higher, sometimes higher than 500 nM. It appeared that AGS cells were more sensitive to CDT than the other two cell lines. We then determined the binding activity of each CDT subunit to CHO-K1 cells by flow cytometry. CdtA bound to CHO-K1 cells at a saturation level of ~10 nM (Fig. 3B). The binding activity of CdtC was higher than that of CdtA at a saturation concentration of ~200 nM; however, CdtB showed no detectable binding activity to CHO-K1 cells. These results indicated that CdtA and CdtC have binding activity to CHO-K1 cells while CdtB did not.

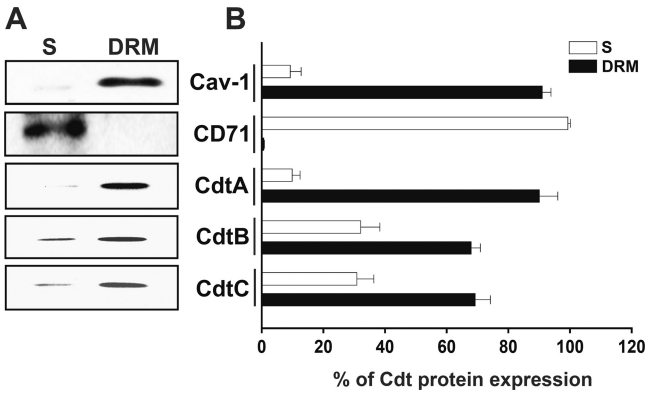

FIG. 7. CdtA and CdtC are enriched in detergent-resistant membrane (DRM) fractions. CHO-K1 cells were left untreated or treated with 10 mM MβCD for 1 h prior to incubation with *C. jejuni* CDT holotoxin (200 nM) for 2 h at 37°C. The cells then were subjected to cold detergent extraction using 1% Triton X-100, followed by centrifugation to separate the DRM and detergent-soluble (S) fractions. (A) Each fraction was subjected to Western blot analysis using antibodies against caveolin-1 and CD71 and individual antisera specific to CdtA, CdtB, and CdtC. The results are representative of one of three independent experiments. (B) The protein expression levels were analyzed using scanning densitometry. The protein expression levels represent the relative distribution (percent) of each protein within the DRM and soluble fractions. MβCD, methyl-β-cyclodextrin.

Cholesterol is required for the association of *C. jejuni* CDT with the cell membrane. To determine whether cholesterol is important for the association of the *C. jejuni* CDT subunits with the membrane, we evaluated the ability of MβCD to deplete cholesterol from cells and membrane rafts (also called the detergent-resistant membrane [DRM]). As shown in Fig. 4A, the cholesterol concentration in total cell lysates and the DRM was decreased as early as 10 min after the treatment of CHO-K1 cells with 10 mM MβCD. Furthermore, the cholesterol levels of total cell lysates and the DRM were reduced in a dose-dependent manner by MβCD treatment for 1 h. The result showed that more than 60 and 90% of the cellular and DRM cholesterol, respectively, was extracted when cells were treated with 10 mM MβCD (Fig. 4B). We then examined the cytotoxic effect of various concentrations of MβCD on CHO-K1 cells; the cells remained essentially viable even when they were treated with 20 mM MβCD for 1 h followed by incubation with lovastatin for a further 24 h (Fig. 4C).

We then assessed the association of the CDT subunits with membrane rafts. CHO-K1 cells first were incubated with 200 nM the individual CDT subunits for 2 h at 4°C. Subsequently, the cells were analyzed by flow cytometry for the presence of CDT proteins on the cell membrane. As shown in Fig. 5 (upper), CdtA and CdtC were associated with the cell membrane. The mean channel fluorescence levels (MCF) for anti-CdtA and anti-CdtC antibodies were 42.4 and 130.0, respectively; however, the MCF for anti-CdtB antibody was only 11.0. When CHO-K1 cells were pretreated with 10 mM MβCD for 1 h, the MCF were reduced for both anti-CdtA (26.4) and anti-CdtC (32.1) antibodies (Fig. 5, lower); however, the MCF of the anti-CdtB (10.2) antibody remained similar to the level of cells not treated with MβCD. We then examined whether cholesterol depletion could affect the binding of CDT holotoxin to

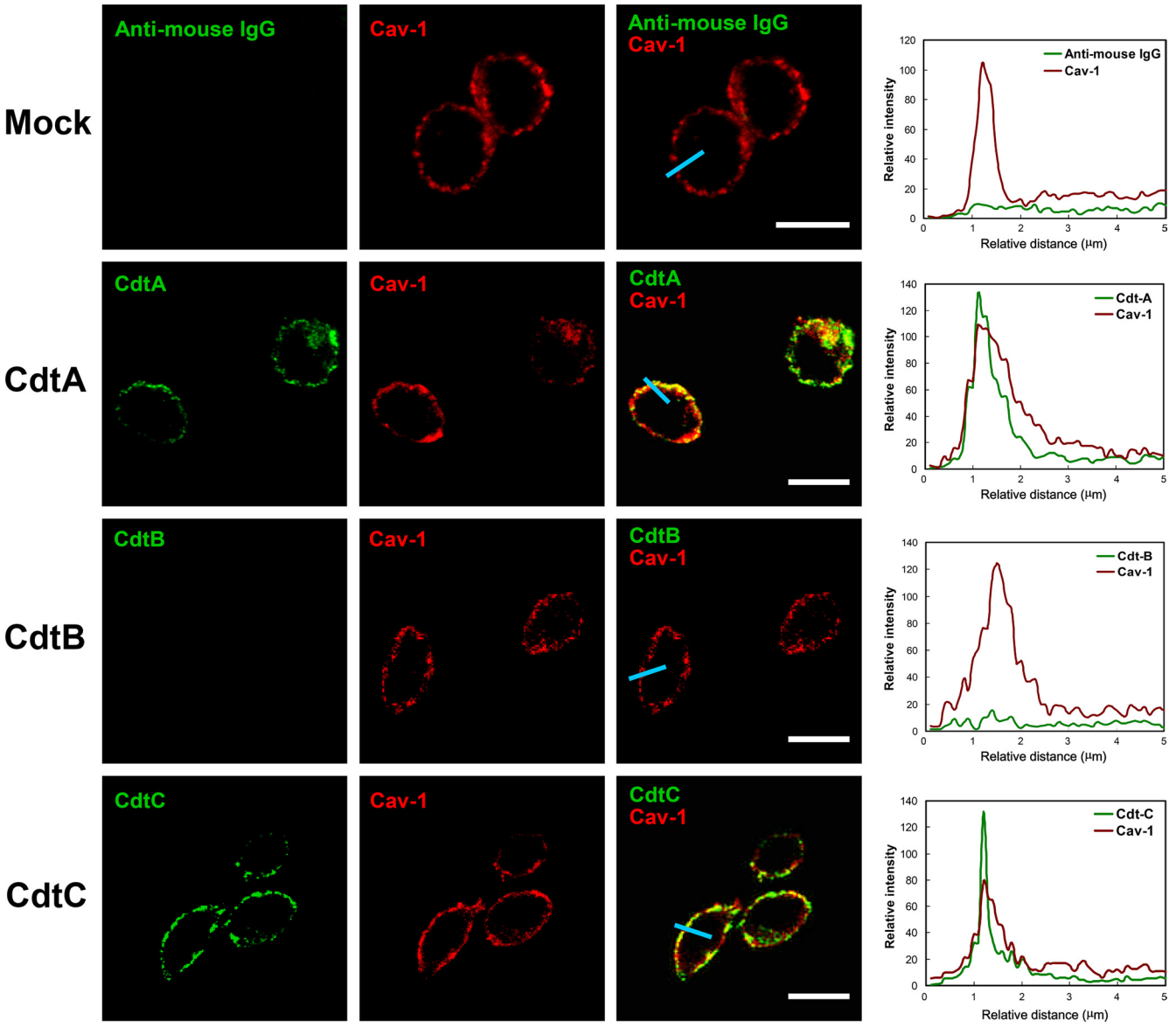

FIG. 8. Association of CdtA and CdtC with membrane rafts. CHO-K1 cells were exposed to medium alone or 200 nM each recombinant *C. jejuni* CDT subunit at 11°C for 1 h. The cells were washed and treated with control preimmune serum or each anti-CDT antiserum and then probed with FITC-conjugated anti-mouse IgG (green). The cells were costained with anti-caveolin-1 and Alexa Fluor 647-conjugated anti-rabbit IgG to visualize the raft microdomains (red) and analyzed by confocal microscopy. The colocalization of each CDT subunit with lipid raft domains appears as yellow in the overlay. Scale bars, 10 μm. The distribution of fluorescence intensity for each CDT subunit and Cav-1 signals across the blue lines were calculated and are presented as line intensity histograms in the right panels. Cav-1, caveolin-1.

cells. Noticeably, compared to the level for the control CHO-K1 cells (Fig. 6, upper), the pretreatment of CHO-K1 cells with MβCD reduced CDT holotoxin binding (Fig. 6, lower). Taken together, these results indicate that both CdtA and CdtC are the key subunits binding to DRM, and the activity of CdtB in holotoxin depends on the binding activity of CdtA and CdtC.

We next analyzed the detergent solubility of membranes from CDT-treated cells to determine whether recombinant *C. jejuni* CDT holotoxin could associate with lipid rafts. CHO-K1 cells were exposed to CDT holotoxin (200 nM each subunit) for 2 h at 37°C. The cells then were collected and treated with ice-cold 1% Triton X-100 for 30 min, followed by gentle centrifugation to separate the DRM and soluble fractions. Western blotting showed that a raft-associated protein, caveolin-1, was enriched in the DRM fraction (Fig. 7). In contrast, a non-raft-associated protein, CD71 (also known as the transferrin receptor), was distributed mainly in the soluble fraction. The localizations of CdtA and CdtC were enriched in the DRM fraction of CHO-K1 cells but not in the soluble fraction (Fig. 7). When cells were exposed to CDT holotoxin, the majority of CdtB was associated with DRM fraction, but a small portion of this protein was found in the soluble fraction. However, when cells were incubated with CdtB alone, CdtB was not detected in the

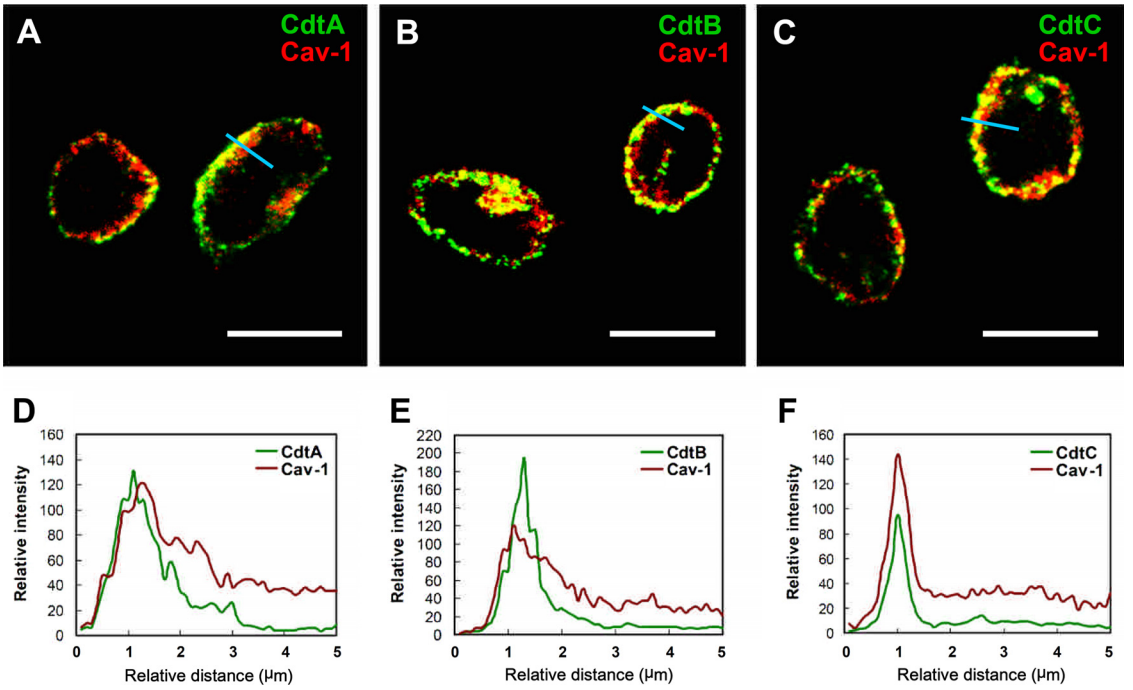

FIG. 9. Localization of CdtB in membrane rafts through the association of CdtA and CdtB with rafts. CHO-K1 cells were exposed to 200 nM CDT holotoxin for 1 h at 11°C. The cells were washed and stained with each anti-CDT antiserum and then probed with FITC-conjugated anti-mouse IgG (green). The cells were costained with anti-caveolin-1 and Alexa Fluor 647-conjugated anti-rabbit IgG to visualize the raft microdomains (red). The stained cells then were analyzed using a confocal microscope. Scale bars, 10 μm. The distribution of fluorescence intensity for individual CDT subunits and Cav-1 signals across the blue lines were calculated and presented as line intensity histograms in the lower panels. Cav-1, caveolin-1.

DRM or soluble fractions (data not shown). These results were consistent with the data presented in Fig. 5 and 6, suggesting that the delivery of *C. jejuni* CdtB requires the association of both CdtA and CdtC subunits with the membrane rafts in target cells.

Delivery of CdtB into cells requires the association of CdtA and CdtC with raft microdomains. We next used confocal microscopy to visualize whether the distribution of *C. jejuni* CDT subunits is raft associated. CHO-K1 cells were incubated with 200 nM the individual CDT subunits at 11°C for 1 h to maintain cell membrane fluidity and prevent internalization. The cells then were stained with preimmune serum and antiserum to CdtA, CdtB, or CdtC. The cells were exposed to an anti-caveolin-1 antibody to identify the membrane raft microdomains. As expected, there was no signal for CDT subunits in untreated CHO-K1 cells, whereas caveolin-1 staining was observed around the plasma membrane (Fig. 8, first row). When cells were treated with each of the CDT subunits at 11°C for 1 h, CdtA (green in Fig. 8, second row) and CdtC (green in Fig. 8, fourth row) colocalized with caveolin-1 (red) on the plasma membrane. In contrast, no CdtB fluorescence could be detected on the plasma membrane (Fig. 8, third row). We then examined CDT holotoxin with confocal microscopy. Imaging analyses showed that CdtA (Fig. 9A) and CdtC (Fig. 9C) colocalized with caveolin-1 (red). In parallel, CdtB was associated with membrane rafts (Fig. 9B). The analysis of the distribution of fluorescence showed that all three CDT subunits colocalized with the membrane raft marker caveolin-1 (Fig. 9D, E, and F). These data were consistent with our findings for CDT binding activity using flow cytometry (Fig. 5 and 6), indicating that CdtA and CdtC not only associate with the membrane but also colocalize with the cholesterol-rich microdomains.

To further test whether CdtB transport to the host cells is dependent on the association of CdtA and CdtC with membrane lipid rafts, cells were exposed to CDT holotoxin (200 nM each subunit) at 37°C for 1 to 6 h. As expected, we first observed the cytoplasmic distribution of CdtB (green) at 2 h and then a clear nuclear distribution after 6 h in cells without MβCD (Fig. 10A, upper). However, the amount of CdtB-associated fluorescence detected at the nucleus was visibly reduced when the cells were pretreated with 10 mM MβCD (Fig. 10A, lower). We then examined whether the nuclear localization of CdtB was dependent on the presence of cholesterol. The cells were pretreated with 10 mM MβCD for 1 h and then exposed to CDT holotoxin for 1 to 6 h at 37°C. As shown in Fig. 10B and C, the nuclear localization of CdtB gradually increased with incubation time in control cells, but its nuclear localization was almost completely blocked in cells with MβCD treatment. Taken together, these observations support the notion that the binding of *C. jejuni* CdtA and CdtC to lipid rafts is important for the delivery of CdtB to target cells.

Cholesterol depletion prevents CDT-induced cell cycle arrest. To determine whether *C. jejuni* CDT-induced cell cycle arrest depended on membrane rafts, we investigated whether the integrity of cholesterol-rich microdomains is essential for CDT holotoxin-induced cell cycle arrest. Only 17% of CHO-K1 control cells were in G_2/M phase, reflecting normal

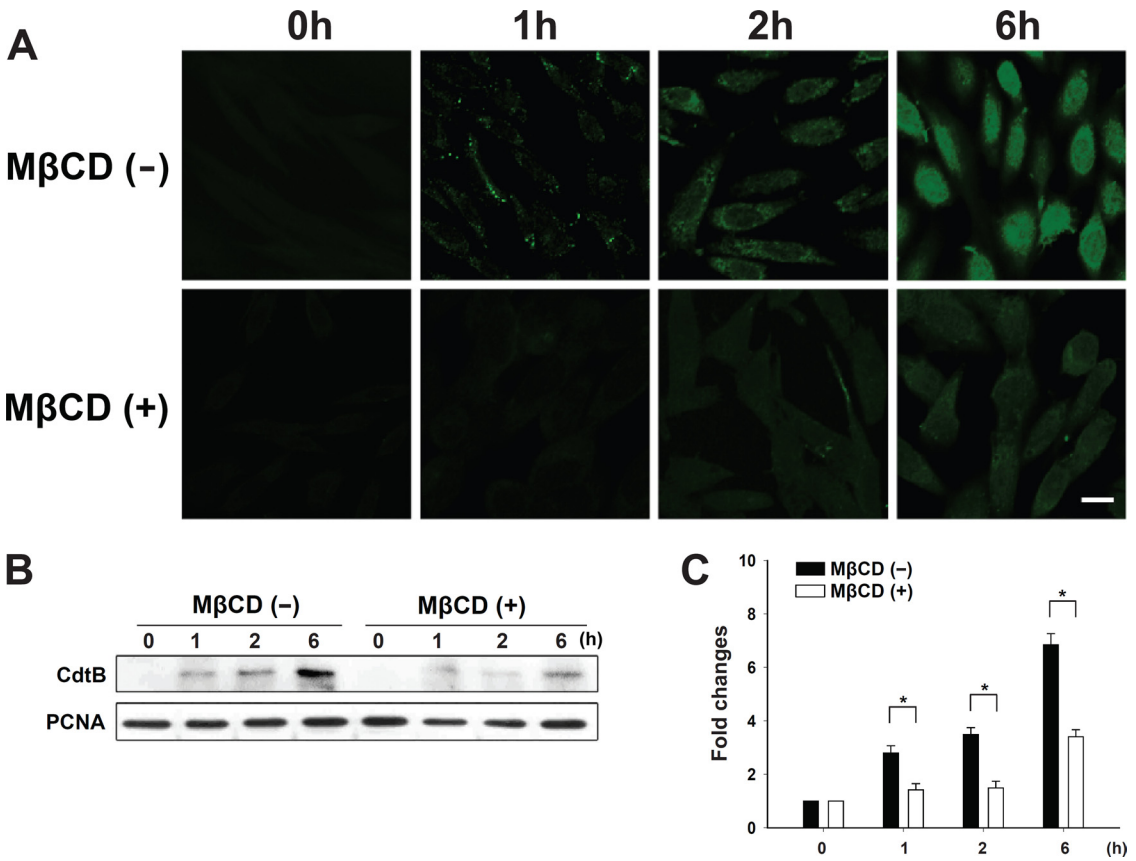

FIG. 10. Depletion of cholesterol prevents the nuclear localization of *C. jejuni* CdtB. (A) CHO-K1 cells were untreated or treated with 10 mM MβCD for 1 h prior to exposure to 200 nM CDT holotoxin at 37°C for the indicated times. The cells were washed and probed with anti-CdtB antiserum, followed by staining with FITC-conjugated anti-mouse IgG. The stained cells then were analyzed by confocal microscopy. Scale bars, 10 μm. (B) The nuclear fraction from cell lysates was prepared from CHO-K1 cells untreated or treated with 10 mM MβCD for 1 h, followed by incubation at 37°C in the presence of CDT holotoxin for the indicated times. CdtB in the nucleus of cell lysates was detected by Western blotting. The results represent three independent experiments. PCNA was used as a loading control for the nuclear fraction of cell lysates. (C) Protein expression levels were analyzed using scanning densitometry. The lower right panel shows the quantitative data for the nuclear CdtB signal. An asterisk indicates $P < 0.05$ compared to results for each untreated MβCD group, as determined by Student's *t* test. MβCD, methyl-β-cyclodextrin; PCNA, proliferating cell nuclear antigen.

cell cycle distribution (Fig. 11A). Cells incubated with 5 or 10 mM MβCD at 37°C for 1 h did not alter the cell cycle distribution, similarly to the control cells (Fig. 11B and C). In the presence of 2 μg/ml ICRF-193, a DNA topoisomerase II inhibitor (3), 60% of cells were accumulated in G_2/M (Fig. 11D), which was used as a positive control for a typical cell cycle arrest.

After pretreating CHO-K1 cells with 0, 5, or 10 mM MβCD at 37°C for 1 h, the cells were incubated with CDT holotoxin for 48 h after the removal of MβCD, and the number of cells arrested in G_2/M clearly decreased in a dose-dependent manner (Fig. 11E to G). Apparently, cholesterol depletion by MβCD, which disrupts the integrity of rafts, also diminishes the activity of CDT, leading to the reduction of G_2/M arrest. Upon the replenishment of cholesterol, the inhibitory effect of MβCD on CDT-induced G_2/M arrest was reversed (Fig. 11H and I). Taken together, these results indicate that the presence of sufficient cholesterol in membrane raft microdomains is required for the activity of *C. jejuni* CDT.

We further analyzed whether the depletion of cholesterol affects CDT-induced cell cycle arrest at the G_2/M phase in other cell types. Three intestinal-derived cell lines (AGS, COLO205, and Caco-2 cells) were employed in this study. Cells were untreated or were pretreated with MβCD for 1 h and then exposed to CDT holotoxin (200 nM) for 48 h. When cells were incubated with CDT holotoxin, levels of cell cycle arrest at G_2/M were significantly higher in CHO-K1, AGS, COLO205, and Caco-2 cells (Fig. 12A). The number of cells arrested in G_2/M was significantly decreased in CHO-K1, AGS, COLO205, and Caco-2 cells upon the pretreatment of cells with MβCD. We further assessed whether the depletion of membrane cholesterol affects the association of the CDT subunits with cell surface. Cells were incubated with 200 nM each CDT subunit and analyzed by flow cytometry for the binding of CDT proteins on the cell membrane. As shown in Fig. 12B, CdtA and CdtC were associated with the cell membrane in all tested cell lines, but CdtB was not. After pretreating cells with MβCD, the binding activity of CdtA and CdtC was reduced significantly in all tested cells. These results indicated that cholesterol is important for the association and intoxication of *C. jejuni* CDT in host cells. Apparently, this

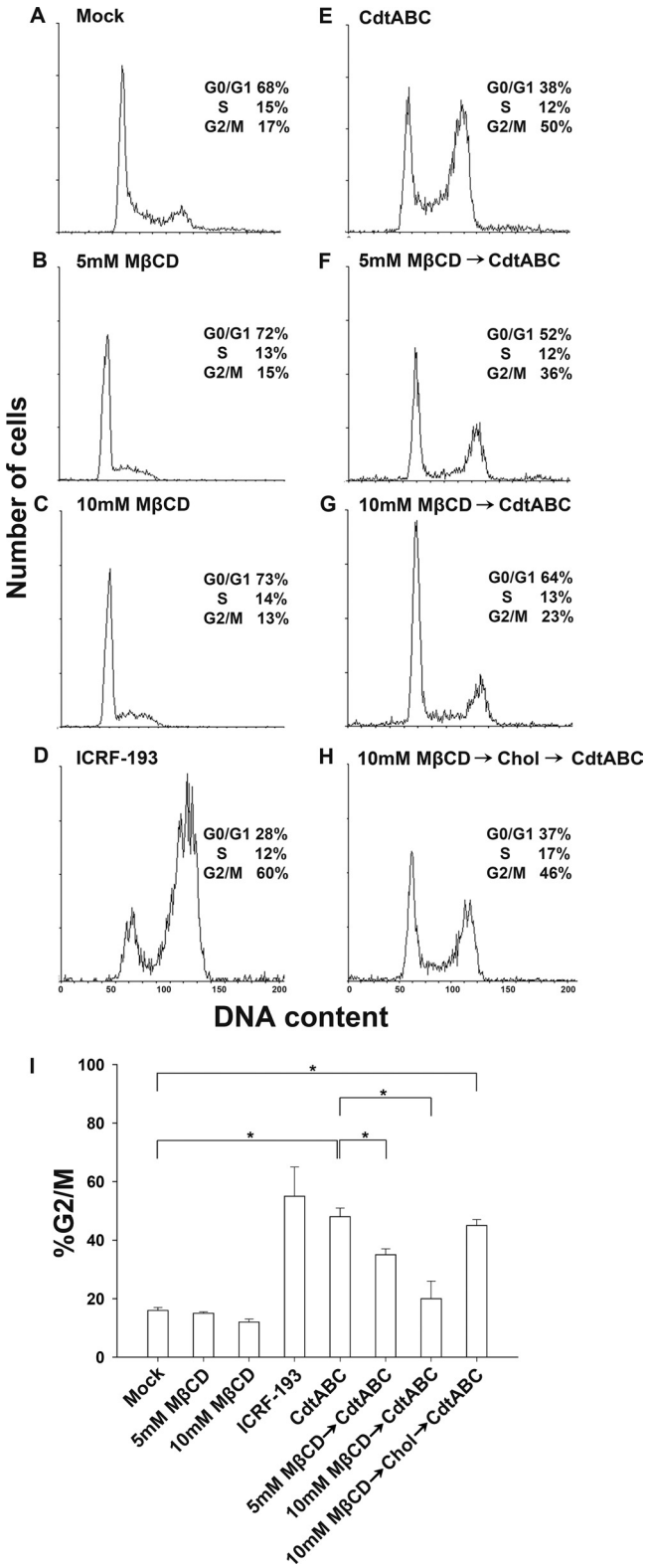

FIG. 11. Sufficient cellular cholesterol is essential for *C. jejuni* CDT-induced cell cycle arrest. CHO-K1 cells were preexposed to medium alone (A, D, and E), 5 mM MβCD (B and F), 10 mM MβCD (C and G), or 10 mM MβCD and replenished with cholesterol (400 μg/ml) for 1 h at 37°C (H). The cells then were incubated for 48 h at 37°C in the presence of medium (A), ICRF-193 (D), and *C. jejuni* CDT holotoxin (E to H). The cell cycle distribution was based on the DNA content, which was analyzed by flow cytometry. The percentage of cells in the G_0/G_1, S, and G_2/M phases of the cell cycle are indicated at the right of each histogram. (I) The percentage of cells in the G_2/M phase were calculated and plotted as intensity histograms. The results represent three independent experiments. An asterisk indicates statistical significance ($P < 0.05$). MβCD, methyl-β-cyclodextrin; Chol, cholesterol.

effect is observed not only in CHO-K1 cells but also in other cells.

DISCUSSION

This study provides evidence that the interaction of *C. jejuni* CdtA and CdtC with cholesterol-rich membrane microdomains is essential for the delivery of CdtB to target cells. The association of *C. jejuni* CDT subunits with membrane lipid rafts was investigated using flow cytometry and biochemical analyses. Our data indicated that both the CdtA and CdtC subunits, but not the CdtB subunit, are capable of binding to the cell membrane, and this binding activity was reduced after cholesterol depletion by MβCD. The CdtB subunit alone neither bound to the cell surface nor associated with lipid rafts; in contrast, CdtB was identified in the DRM fraction from cells incubated with CDT holotoxin. These findings are consistent with the crystal structure of CDT from *H. ducreyi* (38, 39). CdtA and CdtC, which have high homology to ricin proteins, have been shown to have prominent molecular surfaces, an aromatic cluster, and a deep groove that contribute to their membrane interactions (38). Another report indicated that the three CDT subunits from *A. actinomycetemcomitans* form a functional toxin unit on the cell surface which requires complex formation between the CdtA and CdtC subunits (51). These results indicate that the three subunits need to be assembled prior to holotoxin binding to the cell membrane. This is consistent with our observation that, in the presence of holotoxin, *C. jejuni* CdtB was detected predominantly in the DRM fraction of target cells, and this interaction likely is mediated through the association of CdtA and CdtB with lipid rafts.

In this study, we first employed CHO-K1 to study the mechanism of action of CDT holotoxin. Many studies also used this model for the analysis of CDT functions in *Campylobacter* spp. (2, 22, 36, 40), *A. actinomycetemcomitans* (11, 31, 32), *Escherichia coli* (7, 43), and *Shigella dysenteriae* (41) for decades. Thus, it appears that CHO-K1 is a good model for delineating mechanisms of CDT. Nevertheless, we further employed three additional intestinal-derived cell lines (AGS, COLO205, and Caco-2 cells) to determine whether cholesterol plays a crucial role in CDT binding and its activity. Our results conclude that the depletion of cholesterol affects CDT function not only in CHO-K1 cells but also in other cell lines (Fig. 12).

The CRAC region contains the conserved motif $L/V(X)_{1-5}Y(X)_{1-5}R/K$, which is present in proteins that associate with cholesterol (29). A recent report showed that the CdtC subunit of *A. actinomycetemcomitans* contains a CRAC region, which may contribute to the interaction between CdtC and cholesterol (6). Our data and another study (5) indicated that CdtA and CdtC were localized mainly in the cholesterol-rich mi-

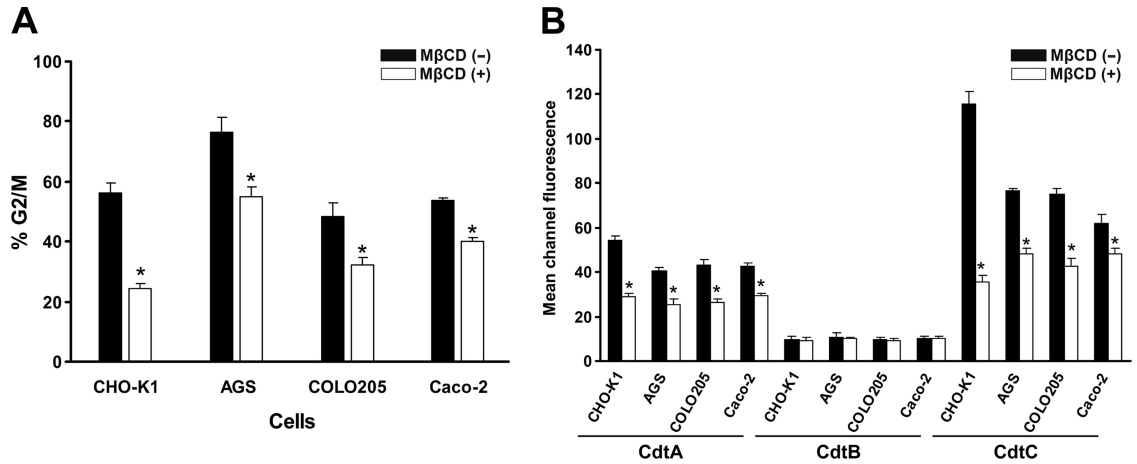

FIG. 12. Cholesterol is important for CDT association and intoxication of cells. (A) Cells from the indicated lines were untreated or treated with 5 mM (for AGS cells) or 10 mM (for other cells) MβCD for 1 h at 37°C, followed by exposure to 200 nM CDT holotoxin for 48 h. Cell cycle distribution was analyzed using flow cytometry. (B) Cells from the indicated lines were untreated or treated with 5 mM (AGS cells) or 10 mM (other cells) MβCD for 1 h at 37°C, followed by incubation with the individual CDT proteins for 2 h at 4°C. The binding activity of each CDT protein was assessed by flow cytometry for FITC fluorescence. The results represent the means and standard deviations from three independent experiments. An asterisk indicates $P < 0.05$ compared to each the untreated MβCD group, as determined by Student's *t* test.

crodomains. We then analyzed the conserved region within the *C. jejuni* CdtC subunit (44), i.e., the amino acid sequence that represents a CRAC-like region (^{77}LPFGYVQFTNPK^{88}) (Fig. 13). *C. jejuni* CdtA also possesses a conserved CRAC-like motif (^{17}LYACSSK^{23}). Thus, these observations indicate that *C. jejuni* CdtA and CdtC contain hypothetical CRAC regions that contribute to their cholesterol-binding activity. However, we did not demonstrate a direct interaction between CdtA/C and cholesterol. Moreover, not all proteins that bind cholesterol have CRAC domains. A recent report indicated that only two amino acids are responsible for the recognition of cholesterol by cytolysin (16). Certainly, further investigation is needed to determine whether the CRAC-like motifs are the most important regions for the interaction of *C. jejuni* CdtA and CdtC with cholesterol.

The importance of cellular cholesterol for another CDT from *A. actinomycetemcomitans* has been well documented by Boesze-Battaglia and colleagues (5). These authors used either confocal microscopy or flow cytometry analysis. Similarly, we also found that CdtA/C of *C. jejuni* could bind to the cell membrane, particularly in the raft microdomains, and this effect was responsible for its toxicity activity. However, we notice some differences of CDT between *A. actinomycetemcomitans* and *C. jejuni* from this study. For example, CDT from *A. actinomycetemcomitans* has been demonstrated to interact with the glycosphingolipids GM1, GM2, and GM3 (35). CHO-K1 cells lack GM2 synthase, which is an upstream enzyme required for GM1 synthesis (49), suggesting that the binding of CDT from *C. jejuni* to the receptors in the cholesterol-enriched microdomains is different from that of *A. actinomycetemcomitans*. Noticeably, in this study we employed cell models resembling the natural host for *C. jejuni*. Therefore, we believe that the outcome of this study reflects the physiological relevance of this toxin.

Several studies have reported that lipid rafts might serve as an entry site for pathogens. For instance, in *Shigella flexneri*, the bacterial invasin IpaB interacts with raft-associated CD44 within specialized membrane microdomains (24). Type 1 fimbriated *E. coli* also was found to be associated with caveolae and lipid raft components (14). Bacteria hijack lipid rafts to mediate the infectious process; similarly, lipid rafts are required for the translocation of cytotoxin-associated gene A

Cdt A amino acid sequence

MQKIIVFILCCFMTFF[17]LYACSSK[23]FENVNPLGRSFGEFEDTDPLKLGLEPTFPTNQEIPSLISGADLV
PITPITPPLTRTSNSANNNAANGINPRFKDEAFNDVLIFENRPAVSDFLTILGPSGAALTVWALAQGNW
IWGYTLIDSKGFGDARVWQLLLYPNDFAMIKNAKTNTCLNAYGNGIVHYPCDASNHAQMWKLIPMSNTA
VQIKNLGNGKCIQAPITNLYGDFHKVFKIFTVECAKKDNFDQQWFLTTPPFTAKPLYRQGEVR

Cdt C amino acid sequence

MKKIITLFFMFITLAFATPTGDLKDFTEMVSIRSLETGIFLSAFRDTSKDPIDQNWNIKEIVLSDELKQ
KDKLADE[77]LPFGYVQFTNPK[88]ESDLCLAILEDGTFGAKSCQDDLKDGKLETVFSIMPTTTSAVQIRSLV
LESDECIVTFFNPNIPIQKRFGIAPCTLDPIFFAEVNELMIITPPLTAATPLE

FIG. 13. Identification of CRAC-like region in CdtA and CdtC. Deduced amino acid sequences of CdtA (upper) and CdtC (lower) are shown. The predicted amino acid motifs containing the putative CRAC-like region are boxed. Numbers indicate the positions of the amino acid residues at each end of the motif. Residues in gray represented conserved pattern in the CRAC-like region.

(CagA) as well as for the delivery of vacuolating cytotoxin (VacA) into host cells following *H. pylori* infection (17, 23, 25, 50). These results suggest that lipid rafts are not only a dynamic structure on the cell membrane but also provide a bacterial entry site for toxin delivery into target cells. Our study suggests that the association of CdtA and CdtC with membrane rafts mediates the action of the toxin more efficiently. This idea is supported by the finding that the *A. actinomycetemcomitans* CdtB subunit exhibits phophatidylinositol-3,4,5-triphosphate (PIP3) phosphatase activity similar to that of phosphatase and tensin homolog deleted on chromosome 10 (PTEN) (30, 52). A previous study found that PTEN normally has a generalized cytosolic and membrane distribution but is recruited into membrane rafts when cells are treated with ceramide (18). We found that both CdtA and CdtC interact with lipid rafts (predominantly localized in cholesterol-rich microdomains) to enhance the association of CdtB with the cell membrane and its subsequent delivery into the cells. This association may be important for the toxin to hijack lipid rafts for the regulation of PIP3 signaling and thereby increase the efficiency of cell intoxication.

In a recent report, Eshraghi et al. presented a comprehensive analysis of the role of glycosylation and cholesterol on the ability of CDTs from several bacterial species, including *A. actinomycetemcomitans*, *C. jejuni*, *E. coli*, and *H. ducreyi*, to intoxicate different cell types (15). The authors found that CDT from *C. jejuni*-induced CHO-K1 cell intoxication was much less efficient than the intoxication of CHO-K1 cells with other CDTs or the intoxication of other cell types with *C. jejuni* CDT. The authors also demonstrated that *C. jejuni* CDT-induced cell cycle arrest of CHO-K1 cells was not influenced by cholesterol loading but was enhanced by inhibiting glycosylation. In contrast, in this study, we showed that cholesterol plays a crucial role in the binding of *C. jejuni* CDT with CHO-K1 cells. This discrepancy may be due to the different concentrations of *C. jejuni* CDT used in these studies. We applied a higher concentration of *C. jejuni* CDT (200 nM) than that used in the study of Eshraghi et al. (50 nM), in which cell cycle arrest in CHO-K1 cells became more apparent under the higher concentration of CDT, suggesting that a higher concentration of CDT is mediated through different mechanisms. Additionally, we used MβCD to deplete cholesterol from lipid rafts and showed the reduced binding activity of CdtA and CdtC, which is different from the method of Eshraghi et al., who added cholesterol directly into cultured cells. Another key question is the specificity of MβCD to cholesterol. The depletion of cholesterol by MβCD also may have extracted other raft-associated molecules, e.g., glycoproteins and gangliosides (42, 53, 56). A previous study indicated that carbohydrate residues are important for CDT binding to cells (33). It is reasonable to speculate that receptor candidates may be removed after treating cells with MβCD; thus, this may explain the influence of MβCD treatment on the cell binding activity of CdtA and CdtC observed in our study.

In conclusion, we demonstrated that membrane cholesterol plays a critical role in the *C. jejuni* CDT intoxication of cells, and CdtA and CdtC were associated with lipid rafts, which are critical for the delivery of CdtB into target cells. The modulation of cellular cholesterol levels may reduce the association of *C. jejuni* CDT with rafts, thereby attenuating the CDT-induced pathogenesis of host cells. The precise molecular mechanism by which CdtA and CdtC interact with cholesterol-rich microdomains will be the subject of future studies. Since CDT is present in various bacterial species, the investigation of the molecular mechanisms underlying cell cycle arrest and eventual death by *C. jejuni* CDT will advance the understanding of the pathogenicity of CDT-producing bacteria. Very likely, this outcome will enhance the development of novel therapeutic strategies to prevent or cure diseases caused by these bacterial pathogens.

ACKNOWLEDGMENTS

This work was supported by the National Science Council, Taiwan (NSC97-2313-B-039-003-MY3, NSC100-2918-I-039-003), China Medical University, Taiwan (CMU98-S-09, CMU98-CT-12), and the Tomorrow Medical Foundation, Taiwan. We thank Tsu-Lan Wu and Ju-Hsin Chia (Department of Laboratory Medicines, Chang Gung Memorial Hospital, Taoyuan, Taiwan) for kindly providing *C. jejuni* and Wan-Chi Lee, Yu-Lun Lu, Pan-Cien Hsu, and Ming-Chun Kuo for expert technical assistance.

We have no conflicts of interest to declare for this work.

REFERENCES

1. **Abrami, L., S. Liu, P. Cosson, S. H. Leppla, and F. G. van der Goot.** 2003. Anthrax toxin triggers endocytosis of its receptor via a lipid raft-mediated clathrin-dependent process. J. Cell Biol. **160:**321–328.
2. **Bag, P. K., T. Ramamurthy, and U. B. Nair.** 1993. Evidence for the presence of a receptor for the cytolethal distending toxin (CLDT) of *Campylobacter jejuni* on CHO and HeLa cell membranes and development of a receptor-based enzyme-linked immunosorbent assay for detection of CLDT. FEMS Microbiol. Lett. **114:**285–291.
3. **Baus, F., V. Gire, D. Fisher, J. Piette, and V. Dulic.** 2003. Permanent cell cycle exit in G2 phase after DNA damage in normal human fibroblasts. EMBO J. **22:**3992–4002.
4. **Blaser, M. J., R. E. Black, D. J. Duncan, and J. Amer.** 1985. *Campylobacter jejuni*-specific serum antibodies are elevated in healthy Bangladeshi children. J. Clin. Microbiol. **21:**164–167.
5. **Boesze-Battaglia, K., et al.** 2006. Cholesterol-rich membrane microdomains mediate cell cycle arrest induced by *Actinobacillus actinomycetemcomitans* cytolethal-distending toxin. Cell Microbiol. **8:**823–836.
6. **Boesze-Battaglia, K., et al.** 2009. Cytolethal distending toxin-induced cell cycle arrest of lymphocytes is dependent upon recognition and binding to cholesterol. J. Biol. Chem. **284:**10650–10658.
7. **Bouzari, S., and A. Varghese.** 1990. Cytolethal distending toxin (CLDT) production by enteropathogenic *Escherichia coli* (EPEC). FEMS Microbiol. Lett. **59:**193–198.
8. **Brown, D., and G. L. Waneck.** 1992. Glycosyl-phosphatidylinositol-anchored membrane proteins. J. Am. Soc. Nephrol. **3:**895–906.
9. **Brown, D. A., and E. London.** 1998. Functions of lipid rafts in biological membranes. Annu. Rev. Cell Dev. Biol. **14:**111–136.
10. **Butzler, J. P., and M. B. Skirrow.** 1979. Campylobacter enteritis. Clin. Gastroenterol. **8:**737–765.
11. **Cao, L., A. Volgina, C. M. Huang, J. Korostoff, and J. M. DiRienzo.** 2005. Characterization of point mutations in the *cdtA* gene of the cytolethal distending toxin of *Actinobacillus actinomycetemcomitans*. Mol. Microbiol. **58:** 1303–1321.
12. **Cope, L. D., et al.** 1997. A diffusible cytotoxin of *Haemophilus ducreyi*. Proc. Natl. Acad. Sci. U. S. A. **94:**4056–4061.
13. **Corry, J. E., and H. I. Atabay.** 2001. Poultry as a source of *Campylobacter* and related organisms. Symp. Ser. Soc. Appl. Microbiol. **2001:**96S–114S.
14. **Duncan, M. J., G. Li, J. S. Shin, J. L. Carson, and S. N. Abraham.** 2004. Bacterial penetration of bladder epithelium through lipid rafts. J. Biol. Chem. **279:**18944–18951.
15. **Eshraghi, A., et al.** 2010. Cytolethal distending toxin family members are differentially affected by alterations in host glycans and membrane cholesterol. J. Biol. Chem. **285:**18199–18207.
16. **Farrand, A. J., S. LaChapelle, E. M. Hotze, A. E. Johnson, and R. K. Tweten.** 2010. Only two amino acids are essential for cytolytic toxin recognition of cholesterol at the membrane surface. Proc. Natl. Acad. Sci. U. S. A. **107:** 4341–4346.
17. **Gauthier, N. C., et al.** 2005. *Helicobacter pylori* VacA cytotoxin: a probe for a clathrin-independent and Cdc42-dependent pinocytic pathway routed to late endosomes. Mol. Biol. Cell **16:**4852–4866.
18. **Goswami, R., D. Singh, G. Phillips, J. Kilkus, and G. Dawson.** 2005. Ceramide regulation of the tumor suppressor phosphatase PTEN in rafts isolated from neurotumor cell lines. J. Neurosci. Res. **81:**541–550.

19. **Guerra, L., et al.** 2005. Cellular internalization of cytolethal distending toxin: a new end to a known pathway. Cell. Microbiol. **7:**921–934.
20. **Hickey, T. E., et al.** 2000. *Campylobacter jejuni* cytolethal distending toxin mediates release of interleukin-8 from intestinal epithelial cells. Infect. Immun. **68:**6535–6541.
21. **Hooper, N. M.** 1999. Detergent-insoluble glycosphingolipid/cholesterol-rich membrane domains, lipid rafts and caveolae (review). Mol. Membr. Biol. **16:**145–156.
22. **Johnson, W. M., and H. Lior.** 1988. A new heat-labile cytolethal distending toxin (CLDT) produced by *Campylobacter* spp. Microb. Pathog. **4:**115–126.
23. **Kuo, C. H., and W. C. Wang.** 2003. Binding and internalization of *Helicobacter pylori* VacA via cellular lipid rafts in epithelial cells. Biochem. Biophys. Res. Commun. **303:**640–644.
24. **Lafont, F., G. Tran Van Nhieu, K. Hanada, P. Sansonetti, and F. G. van der Goot.** 2002. Initial steps of *Shigella* infection depend on the cholesterol/sphingolipid raft-mediated CD44-IpaB interaction. EMBO J. **21:**4449–4457.
25. **Lai, C. H., et al.** 2008. Cholesterol depletion reduces *Helicobacter pylori* CagA translocation and CagA-induced responses in AGS cells. Infect. Immun. **76:**3293–3303.
26. **Lara-Tejero, M., and J. E. Galan.** 2000. A bacterial toxin that controls cell cycle progression as a DNase I-like protein. Science **290:**354–357.
27. **Lara-Tejero, M., and J. E. Galan.** 2001. CdtA, CdtB, and CdtC form a tripartite complex that is required for cytolethal distending toxin activity. Infect. Immun. **69:**4358–4365.
28. **Lara-Tejero, M., and J. E. Galan.** 2002. Cytolethal distending toxin: limited damage as a strategy to modulate cellular functions. Trends Microbiol. **10:**147–152.
29. **Li, H., and V. Papadopoulos.** 1998. Peripheral-type benzodiazepine receptor function in cholesterol transport. Identification of a putative cholesterol recognition/interaction amino acid sequence and consensus pattern. Endocrinology **139:**4991–4997.
30. **Maehama, T., and J. E. Dixon.** 1999. PTEN: a tumour suppressor that functions as a phospholipid phosphatase. Trends Cell Biol. **9:**125–128.
31. **Mao, X., and J. M. DiRienzo.** 2002. Functional studies of the recombinant subunits of a cytolethal distending holotoxin. Cell Microbiol. **4:**245–255.
32. **Mayer, M. P., L. C. Bueno, E. J. Hansen, and J. M. DiRienzo.** 1999. Identification of a cytolethal distending toxin gene locus and features of a virulence-associated region in *Actinobacillus actinomycetemcomitans*. Infect. Immun. **67:**1227–1237.
33. **McSweeney, L. A., and L. A. Dreyfus.** 2005. Carbohydrate-binding specificity of the *Escherichia coli* cytolethal distending toxin CdtA-II and CdtC-II subunits. Infect. Immun. **73:**2051–2060.
34. **Mead, P. S., et al.** 1999. Food-related illness and death in the United States. Emerg. Infect. Dis. **5:**607–625.
35. **Mise, K., et al.** 2005. Involvement of ganglioside GM3 in G(2)/M cell cycle arrest of human monocytic cells induced by *Actinobacillus actinomycetemcomitans* cytolethal distending toxin. Infect. Immun. **73:**4846–4852.
36. **Mizuno, K., K. Takama, and S. Suzuki.** 1994. Characteristics of cytotoxin produced by *Campylobacter jejuni* strains. Microbios **78:**215–228.
37. **Montfort, W., et al.** 1987. The three-dimensional structure of ricin at 2.8 A. J. Biol. Chem. **262:**5398–5403.
38. **Nesić, D., Y. Hsu, and C. E. Stebbins.** 2004. Assembly and function of a bacterial genotoxin. Nature **429:**429–433.
39. **Nesic, D., and C. E. Stebbins.** 2005. Mechanisms of assembly and cellular interactions for the bacterial genotoxin CDT. PLoS Pathog. **1:**e28.
40. **Ohya, T., K. Tominaga, and M. Nakazawa.** 1993. Production of cytolethal distending toxin (CLDT) by *Campylobacter fetus* subsp. fetus isolated from calves. J. Vet. Med. Sci. **55:**507–509.
41. **Okuda, J., H. Kurazono, and Y. Takeda.** 1995. Distribution of the *cytolethal distending toxin A gene* (*cdtA*) among species of *Shigella* and *Vibrio*, and cloning and sequencing of the *cdt* gene from *Shigella dysenteriae*. Microb. Pathog. **18:**167–172.
42. **Orlandi, P. A., and P. H. Fishman.** 1998. Filipin-dependent inhibition of cholera toxin: evidence for toxin internalization and activation through caveolae-like domains. J. Cell Biol. **141:**905–915.
43. **Orth, D., K. Grif, M. P. Dierich, and R. Wurzner.** 2006. Cytolethal distending toxins in Shiga toxin-producing *Escherichia coli*: alleles, serotype distribution and biological effects. J. Med. Microbiol. **55:**1487–1492.
44. **Parkhill, J., et al.** 2000. The genome sequence of the food-borne pathogen *Campylobacter jejuni* reveals hypervariable sequences. Nature **403:**665–668.
45. **Pérès, S. Y., et al.** 1997. A new cytolethal distending toxin (CDT) from *Escherichia coli* producing CNF2 blocks HeLa cell division in G2/M phase. Mol. Microbiol. **24:**1095–1107.
46. **Pickett, C. L., et al.** 1996. Prevalence of cytolethal distending toxin production in *Campylobacter jejuni* and relatedness of *Campylobacter* sp. *cdtB* gene. Infect. Immun. **64:**2070–2078.
47. **Rasrinaul, L., et al.** 1988. Foods as a source of enteropathogens causing childhood diarrhea in Thailand. Am. J. Trop. Med. Hyg. **39:**97–102.
48. **Ricci, V., et al.** 2000. High cell sensitivity to *Helicobacter pylori* VacA toxin depends on a GPI-anchored protein and is not blocked by inhibition of the clathrin-mediated pathway of endocytosis. Mol. Biol. Cell **11:**3897–3909.
49. **Rosales Fritz, V. M., J. L. Daniotti, and H. J. Maccioni.** 1997. Chinese hamster ovary cells lacking GM1 and GD1a synthesize gangliosides upon transfection with human GM2 synthase. Biochim. Biophys. Acta **1354:**153–158.
50. **Schraw, W., Y. Li, M. S. McClain, F. G. van der Goot, and T. L. Cover.** 2002. Association of *Helicobacter pylori* vacuolating toxin (VacA) with lipid rafts. J. Biol. Chem. **277:**34642–34650.
51. **Shenker, B. J., et al.** 2005. Induction of cell cycle arrest in lymphocytes by *Actinobacillus actinomycetemcomitans* cytolethal distending toxin requires three subunits for maximum activity. J. Immunol. **174:**2228–2234.
52. **Shenker, B. J., et al.** 2007. A novel mode of action for a microbial-derived immunotoxin: the cytolethal distending toxin subunit B exhibits phosphatidylinositol 3,4,5-triphosphate phosphatase activity. J. Immunol. **178:**5099–5108.
53. **Simons, K., and D. Toomre.** 2000. Lipid rafts and signal transduction. Nat. Rev. Mol. Cell Biol. **1:**31–39.
54. **Simons, M., et al.** 2002. Overexpression of the myelin proteolipid protein leads to accumulation of cholesterol and proteolipid protein in endosomes/lysosomes: implications for Pelizaeus-Merzbacher disease. J. Cell Biol. **157:**327–336.
55. **Sugai, M., et al.** 1998. The cell cycle-specific growth-inhibitory factor produced by *Actinobacillus actinomycetemcomitans* is a cytolethal distending toxin. Infect. Immun. **66:**5008–5019.
56. **Wolf, A. A., et al.** 1998. Ganglioside structure dictates signal transduction by cholera toxin and association with caveolae-like membrane domains in polarized epithelia. J. Cell Biol. **141:**917–927.
57. **Wu, T. L., et al.** 2002. Molecular epidemiology of nalidixic acid-resistant campylobacter isolates from humans and poultry by pulsed-field gel electrophoresis and flagellin gene analysis. Epidemiol. Infect. **129:**227–231.
58. **Young, V. B., K. A. Knox, and D. B. Schauer.** 2000. Cytolethal distending toxin sequence and activity in the enterohepatic pathogen *Helicobacter hepaticus*. Infect. Immun. **68:**184–191.
59. **Zheng, J., J. Meng, S. Zhao, R. Singh, and W. Song.** 2008. *Campylobacter*-induced interleukin-8 secretion in polarized human intestinal epithelial cells requires *Campylobacter*-secreted cytolethal distending toxin- and Toll-like receptor-mediated activation of NF-kappaB. Infect. Immun. **76:**4498–4508.

Editor: S. R. Blanke